

Research Paper

# Steady Gyrostatic Nanofluid Flow past a Permeable Stretching/shrinking Sheet with Velocity Slip Condition using the Nanofluid Model Proposed by Buongiorno

Waqar Khan Usafzai<sup>1</sup>, Ioan Pop<sup>2</sup> , Emad H. Aly<sup>3</sup>

<sup>1</sup> School of Mathematics and Physics, Nanjing Institute of Technology, Nanjing, China

<sup>2</sup> Department of Mathematics, Faculty of Mathematics and Computer Science, Babes-Bolyai University, Cluj-Napoca, Romania

<sup>3</sup> Department of Mathematics, Faculty of Education, Ain Shams University, Roxy, Cairo, Egypt

Received November 30 2023; Revised January 04 2024; Accepted for publication January 26 2024.

Corresponding author: I. Pop (popm.ioan@yahoo.co.uk)

© 2024 Published by Shahid Chamran University of Ahvaz

**Abstract.** A detailed analysis, is presented in this paper, for the steady gyrostatic nanofluid flow past a permeable stretching/shrinking sheet with slip condition using the nanofluid model proposed by Buongiorno. The microorganisms are imposed into the nanofluid to stabilize the nanoparticles to suspend due to a phenomenon called bioconvection. Considering appropriate similarity transformations, the five partial differential equations of mass conservation, momentum, thermal energy and microorganisms are reduced to a set of four ordinary (similar) differential equations with coupled linear boundary conditions. These equations were both analytical and numerical solved using Runge-Kutta-Fehlberg technique. The influences of important physical parameters, such as, Prandtl number  $Pr$ , the Schmidt number  $Sc$ , the bioconvection Péclet number  $Pe$ , the Brownian motion parameter  $Nb$ , the thermophoresis parameter  $Nt$  and the stretching/shrinking parameter  $\lambda$  on the skin friction coefficient  $C_f$  and the local Nusselt number  $Nu_x$ , as well as on the velocity, temperature and gyration profiles, are interpreted through graphs and tables. Further, multiple (dual, upper and lower branch solutions) are found for the governing similarity equations and the upper branch solution expanded with higher values of the suction parameter. It can be confirmed that the lower branch solution is unstable. It is found that the bioconvection parameters have strong influence towards the reduced skin friction coefficient, reduced heat transfer, velocity and density of motile microorganism's transport rates.

**Keywords:** Gyrostatic nanofluid, stretching/shrinking sheet, slip condition, analytical solutions, multiple solutions.

## 1. Introduction

Heat transfer is essential in various applications, e.g., power generation and electronic devices. The thermal management of such equipment is necessary for the development of an efficient heat transfer medium. Several years ago, nanofluids were designed to fulfill the requirements for better heat-conducting qualities in traditional fluids. Nanofluid is mixture of nanosized particles suspended in a base fluid that has greater thermal conductivity in comparison with the base fluid. The rate of heat transfer in industrial processes and the nuclear reactions is due to its higher thermal conductivity. The heat conduction has a great importance in many industrial heating or cooling equipment's. Choi in 1995 [1] at Argonne National Laboratory, USA, was the first researcher who gave life to this concept of nanofluids. It is well known that mixing nanoparticle in a fluid involve a change in the liquid's thermophysical and optical properties such as thermal conductivity. But conventional fluids do not allow to grow so efficiently the intensified fluid flow and heat transfer. Nanofluids have received much attention because they are potentially used as a thermophysical heat transfer fluid. Here we recall some practical applications of nanofluids, such as cooling engine components in the automotive industry, their property to convert solar energy into thermal energy, and improving absorption and storage capacity in solar panels, building heating systems, solar drying devices, and many others (see the papers by Shah et al. [2], Raza et al. [3], Khan et al. [4], Ahmad et al. [5], the review papers by Mahian et al. [6, 7], Pop et al. [8], and in the books by Minea [9] and Merkin et al. [10]).

An extensive description of two-phase convective transport in nanofluids was made by Buongiorno [11], who considered seven slip mechanisms: inertia, Brownian diffusion, thermophoresis, diffusion phoresies, Magnus effect, fluid drainage and gravity settling. Finally, he concluded that in the absence of turbulent effects it is the Brownian diffusion and the thermophoresis that are the most important. Several issues are involved while studying heat transfer enhancement utilizing nanofluids. Combination of buoyancy forces due to temperature gradient and forced convection due to shear, results in a free or mixed convection heat



transfer, is a complex phenomenon due to the interaction of these forces. In this model, the Brownian motion and thermophoresis enter to produce their effects directly into the equations expressing the conservation of energy and nanoparticles, so that the temperature and the particle density are coupled in a particular way, and that results in the thermal and concentration buoyancy effects being coupled in the same way.

Bioconvection is a phenomenon that occurs when convection instability is induced by up swimming microorganisms that are heavier than water. Due to up swimming, the microorganisms involved, such as gyrotactic microorganisms like algae, tend to concentrate in the upper portion of the fluid layer thus causing a top-heavy density stratification that often becomes unstable (see Pedley et al. [12], and Kuznetsov and Gang [13]). It seems that Kuznetsov and Avramenko [14], first introduced the bioconvection problem containing tiny solid particles as well as gyrotactic microorganisms. The study by Kuznetsov [15] has laid the ground work for the theory to describe the early stage of convection instability, or also known as nanofluid bioconvection, which is induced by simultaneous effects produced by oxytactic microorganisms, nanoparticles, and vertical temperature variation. There are mainly two types of up swimming micro-organisms that are generally applied in bioconvection experiments: bottom-heavy algae and firm oxytactic bacteria. The bioconvection structures created by microorganisms are similar although, the mechanisms of direction are different (see Pedley et al. [12]). This guides to the development of hydrodynamic instability under definite circumstances. The motile micro-organisms are self-urged which enlarges the denseness of the primary fluid by swimming toward a particular direction within the liquid in attraction to stimulus such as oxygen, daylight, gravity whereas nanoparticles cannot swim. For practical purpose, at fundamental level, the nature of suspensions carrying both nanoparticles and self-swimming microorganisms in microsystems must be understood. By having bioconvection motion in the nanofluids, the mixing nanoparticles issue could be resolved, and could enhance mass transfer in microvolumes (see Kuznetsov [16]). On the other hand, adding microorganisms to a nanofluid increases its stability as a suspension and could avoid nanoparticles from agglomerating and aggregating (Kuznetsov [16]). Aziz et al. [17] have numerically studied the free convection boundary layer flow past a horizontal flat plate in nanofluid containing gyrotactic microorganisms, and they found that the bioconvection parameters have strongly influenced. Tham et al. [18] investigated the mixed convection flow over a solid sphere embedded in a porous medium filled by a nanofluid containing gyrotactic microorganisms. Xu and Pop [19], studied the mixed convection flow of a nanofluid over a stretching surface with uniform free stream in the presence of both nanoparticles and gyrotactic microorganisms.

The flow due to a stretching/shrinking surface is an important problem in many engineering processes with application in industries such as extrusion processes, expanding balloons, extension of pseudopods, glass blowing, hot rolling, wire drawing, paper production, glass blowing, plastic films drawing, glass-fiber production, etc. The quality of the final product depends on the rate of heat transfer at the stretching surface (Fisher [20]). The case of a viscous fluid due to a shrinking surface has been first studied by Miklavcic and Wang [21]. In most cases, such as stretching of elastic materials, the velocity is linearly proportional to the distance and similarity solutions for viscous flow may exist. It was shown that mass suction is required to maintain the flow over a shrinking sheet. The flow induced by a shrinking sheet with constant velocity or power-law velocity distribution is investigated by Fang et al. [22], Rohni et al. [23], etc. Aman et al. [24] studied the problem of mixed convection flow of a nanofluid containing gyrotactic microorganisms over a stretching/shrinking sheet in the presence of magnetic field. Goldstein [25] has pointed out that the new type of shrinking sheet flow is essentially a backward flow, and it shows physical phenomena quite distinct from the stretching flow case.

The main assumption of the Navier–Stokes concept is the no-slip border rule. This rule does not apply in some cases, such as in liquids, polymer solutions, emulsions, and foams. Several researchers studied no slip boundary conditions on fluid flow phenomena. However, some fluids show macroscopic slip, like liquid polymers, foams, and emulsions. Fluid flows in which slip effect are dominant are applicable in many medical applications such as interior body cavities and many industrial and engineering processes. Several researchers studied no slip boundary conditions on fluid flow phenomena. Fluid flows in which slip effect are dominant are applicable in many medical applications such as interior body cavities and many industrial and engineering processes (see Al-Zubaidi et al. [26]). Mabood et al. [27] followed the research work of Navier on slip conditions they investigated the effect of multiple slip on a stretching sheet in a steady flow. They stated that by raising the velocity slip parameter wall friction reduces. The slip condition was first introduced by Navier [28] and then developed by Maxwell [29]. The fluid velocity along the wall differs from the velocity of the moving wall and this difference is proportional to the velocity gradient. This boundary condition was generalized by Smolukhovskiy [30], who showed that for non-isothermal flows the fluid velocity can also change due to the inhomogeneous wall temperature. On the other hand, he found that in this case there is also a temperature slip on the wall.

The flow and heat transfer past a stretching/shrinking surface are considered to be a vast area for the researchers and scientists. Modification in the stretching/shrinking velocities leads to arise many real-life processes, such as rubber sheet, stretching of plastic films, paper production, etc. The impacts of variations in the stretching/shrinking parameter and the volume fraction of nanoparticles are important aspects of nanofluid flow, specifically on the skin friction, Nusselt number (which relates to heat transfer), velocity profiles and the temperature profiles. Using appropriate transformation, the partial differential equations are reduced to a system of ordinary (similar) differential equations, which is solved both analytic and numerical. Numeric findings reveal that the value of the skin friction exhibits variations based on the magnitude of the stretching/shrinking parameter. Moreover, in the specific context of the flow problem being studied, the heat conduction efficiency of nanofluid surpasses that of the hybrid nanofluid. Within a specific interval of the shrinking/stretching parameter, the system yields three distinct solutions. Through an examination of the temporal stability of the solutions, it was determined that only one of them remained stable and physically realisable in practice.

The present paper aims to present a detailed analysis for the gyrostatic nanofluid past a permeable stretching/shrinking sheet with slip condition using the nanofluid model proposed by Buongiorno [11]. The microorganisms are imposed into the nanofluid to stabilize the nanoparticles to suspend due to a phenomenon called bioconvection.

A thorough examination of the published papers on gyrostatic nanofluid flow past a permeable stretching/shrinking sheet with velocity slip is only conceivable to a limited extent. To the best of our knowledge, no previous studies have looked into the boundary layer flow and heat transfer on this topic. Henceforth, motivated by the published papers by Pedley et al. [12], Kuznetsov [15,16], and Xu and Pop [19], the goal of this study is to broaden the research on gyrostatic fluid by employing the nanofluid model proposed by Buongiorno [11], and the influences of important physical parameters, such as, Prandtl number  $Pr$ , the Schmidt number  $Sc$ , the bioconvection Péclet number  $Pe$ , the Brownian motion parameter  $Nb$ , the thermophoresis parameter  $Nt$  and the stretching/shrinking parameter  $\lambda$  on the skin friction coefficient  $C_f$  and the local Nusselt number  $Nu_x$ . The governing boundary layer equations were both analytical and numerical solved using Runge-Kutta-Fehlberg technique. In such a case, this research would like to examine, for the first time, the effect of these parameters on gyrostatic nanofluid flow. Comparative results were obtained for a specific case, disclosing a good correlation with two papers from the open literature. Multiple solutions aroused, an analysis of the stability of the solutions demonstrate the physical interpretations of the generated results. This significant engagement is important and could assist in advancing industrial development, particularly in the operations and manufacturing industries, for example, the transpiration cooling of a re-entry spatial vehicle.



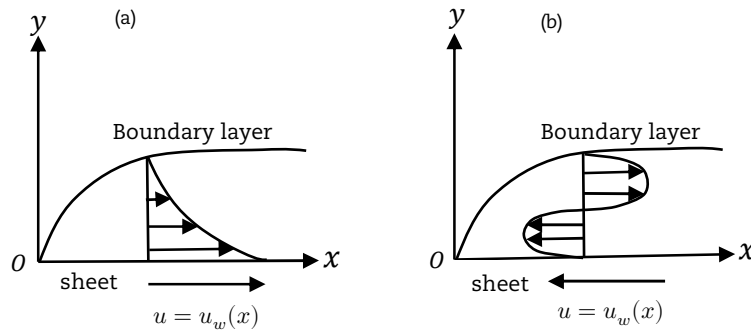


Fig. 1. Physical model and coordinate system: (a) Stretching sheet (b) Shrinking sheet.

## 2. Mathematical Model

Consider the steady gyrostatic nanofluid past a permeable stretching/shrinking sheet with slip condition using the nanofluid model proposed by Buongiorno [11], as shown in Fig. 1, where  $(x, y)$  are the Cartesian coordinates with the  $x$  – axis measured along the sheet and  $y$  – axis is normal to it, the flow being at  $y \geq 0$ .

The appropriate partial differential equations are: the mass conservation, the momentum, energy and gyration, that can be written in Cartesian coordinates as (see Merkin et al. [10])

$$\frac{\partial u}{\partial x} + \frac{\partial v}{\partial y} = 0 \tag{1}$$

$$u \frac{\partial u}{\partial x} + v \frac{\partial u}{\partial y} = \nu \frac{\partial^2 u}{\partial y^2} \tag{2}$$

$$u \frac{\partial T}{\partial x} + v \frac{\partial T}{\partial y} = \alpha \frac{\partial^2 T}{\partial y^2} + \tau \left[ \frac{\partial T}{\partial y} \frac{\partial C}{\partial y} + \frac{D_T}{T_\infty} \left( \frac{\partial T}{\partial y} \right)^2 \right] \tag{3}$$

$$u \frac{\partial C}{\partial x} + v \frac{\partial C}{\partial y} = D_B \frac{\partial^2 C}{\partial y^2} + \frac{D_T}{T_\infty} \left( \frac{\partial T}{\partial y} \right)^2 \tag{4}$$

$$u \frac{\partial N}{\partial x} + v \frac{\partial N}{\partial y} + \frac{b W_c}{C_0} \frac{\partial}{\partial y} \left( N \frac{\partial C}{\partial y} \right) = D_n \frac{\partial^2 N}{\partial y^2} \tag{5}$$

subject to the boundary conditions:

$$\left. \begin{aligned} v = v_w, \quad U_w(x) = u_w(x) + K_1 \frac{\partial u}{\partial y} = c x + K_1 \frac{\partial u}{\partial y}, \\ T = T_w, \quad C = C_0, \quad N = N_w, \\ u = u_e(x) \rightarrow 0, \quad T \rightarrow T_\infty, \quad C \rightarrow 0, \quad N \rightarrow 0 \quad \text{as } y \rightarrow \infty \end{aligned} \right\} \text{ at } y = 0 \tag{6}$$

Here  $(u, v)$  are the velocity components along  $(x, y)$  – axes,  $u_w(x) = cx$  is the stretching/shrinking velocity of the sheet with  $c > 0$  for the stretching,  $c < 0$  for the shrinking and  $c = 0$  for the static sheet,  $T$  is the temperature of the nanofluid,  $C$ , is the nanoparticle concentration,  $N$  is the concentration of microorganism,  $b$  is the constant chemotaxis,  $W_c$  is the maximum cell swimming speed (the product of  $bW_c$  is constant thermal diffusivity,  $D_B$  is the Brownian diffusion coefficient,  $D_T$  is the thermophoretic diffusion coefficient,  $D_n$  is the diffusivity of microorganism,  $\tau = (\rho C_p)_p / (\rho C_p)_f$ , where  $(\rho C_p)_p$  is the effective heat capacity of the nanoparticles material,  $(\rho C_p)_f$  is the heat capacity of the fluid,  $C_p$  is the heat capacity at constant pressure, a constants,  $\alpha$  is the thermal diffusivity,  $\nu$  is the kinematic viscosity,  $K_1$  is the slip factor.

Following Tham et al. [18], we introduce the similarity variables:

$$\left. \begin{aligned} u = a x f'(\eta), \quad v = -\sqrt{a \nu_f} f(\eta), \quad \theta(\eta) = \frac{T - T_\infty}{T_w - T_\infty}, \\ g(\eta) = \frac{C}{C_0}, \quad h(\eta) = \frac{N}{N_w}, \quad \eta = y \sqrt{\frac{a}{\nu_f}} \end{aligned} \right\} \tag{7}$$

where  $a$  is a positive constant.

Substitution (7) into Eqs. (2) to (5), they are reduced then to ordinary (similarity) differential equations:

$$f''' + f f'' - f'^2 = 0 \tag{8}$$

$$\frac{1}{Pr} \theta'' + f \theta' + Nb g' \theta' + Nt \theta'^2 = 0 \tag{9}$$

$$\frac{1}{Sc} g'' + \frac{Nb}{Nt} \theta'' + f g' = 0 \tag{10}$$



$$h'' + Sc fh' - Pe (g'h' + h g'') = 0 \quad (11)$$

subject to the boundary conditions:

$$\left. \begin{aligned} f(0) = S, \quad f'(0) = \lambda + K f''(0), \quad \theta(0) = 1, \quad g(0) = 1, \quad h(0) = 1 \\ f'(\eta) \rightarrow 0, \quad \theta(\eta) \rightarrow 0, \quad g(\eta) \rightarrow 0, \quad h \rightarrow 0 \quad \text{as } \eta \rightarrow \infty \end{aligned} \right) \quad (12)$$

where  $\lambda = c/a$  is the stretching/shrinking parameter, with  $\lambda > 0$  for the stretching,  $\lambda < 0$  for the shrinking and  $\lambda = 0$  for the static sheet.

In the above equations  $Pr$  is the Prandtl number,  $Sc$  is the Schmidt number,  $Pe$  is the bioconvection Péclet number,  $Nb$  is the Brownian motion parameter,  $Nt$  is the thermophoresis parameter,  $K$  is the velocity slip parameter, which are defined as:

$$\left. \begin{aligned} Pr = \frac{\alpha}{\nu}, \quad Le = \frac{\nu}{D_B}, \quad Sc = \frac{\nu}{D_n}, \quad Pe = \frac{b W_c}{D_n}, \quad Nb = \frac{\tau D_B (C_w - C_\infty)}{\nu} \\ Nt = \frac{\tau D_T (T_w - T_\infty)}{\nu T_\infty}, \quad K = K_1 \sqrt{\frac{a}{\nu}} \end{aligned} \right) \quad (13)$$

The physical quantities of interest are the skin friction coefficient  $C_f$  and the local Nusselt number  $Nu_x$ , which are defined as:

$$C_f = \frac{\nu}{u_w^2(x)} \left( \frac{\partial u}{\partial y} \right)_{y=0}, \quad Nu_x = \frac{x}{T_w - T_\infty} \left( - \frac{\partial T}{\partial y} \right)_{y=0} \quad (14)$$

Substituting (7) into (14), we obtain:

$$Re_x^{1/2} C_f = f''(0), \quad Re_x^{-1/2} Nu_x = -\theta'(0) \quad (15)$$

where  $Re_x = u_w(x)x/\nu$  is the local Reynolds number.

### 3. Exact Analytical Solutions

The obtained analytical solutions are found to be in perfect line with the numerical computations. Besides this, exact solutions point to the existence of dual solutions for the shrinking case, were not detected from the numerical studies up to date. The existence of such exact solutions and their parameter domain, which depends on the wall suction or injection are successfully studied here.

#### 3.1. Viscous fluid

In this case, Eq. (8) along with the boundary conditions (12) for  $f(\eta)$  become:

$$\left. \begin{aligned} f''' + ff'' - f'^2 = 0, \\ f(0) = S, \quad f'(0) = \lambda + K f''(0), \quad f'(\eta) \rightarrow 0 \quad \text{as } \eta \rightarrow \infty \end{aligned} \right) \quad (16)$$

Usafzai et al. [32-34], has shown that this boundary value problem, has the following exact analytical solution:

$$f(\eta) = S + \frac{\lambda}{\beta(1 + K\beta)} (1 - e^{-\beta\eta}) \quad (17)$$

where the quantity  $\beta$  is the effective distance parameter, and for physical solutions to hold,  $\beta > 0$ , also responsible for the existence of multiple solutions. It is given by:

$$K\beta^3 + (1 - KS)\beta^2 - S\beta - \lambda = \beta^3 + a_2\beta^2 + a_1\beta + a_0, \quad (18)$$

where  $a_2 = (1 - KS)/K$ ,  $a_1 = -S/K$  and  $a_0 = -\lambda/K$ .

Equation (18) under the transformation  $t = \beta + a_2/3$  can be reduced into the following depressed cubic:

$$t^3 + pt + q = 0, \quad (19)$$

where  $p = a_1 - a_1^2/3$ , and  $q = 2a_2^3/27 - a_1a_2/3 + a_0$ .

The solutions of the depressed cubic in terms of  $\beta$  are listed as follows:

$$\begin{aligned} \beta_1 &= \frac{(KS - 1)}{K} - \frac{\left(\frac{2}{3}\right)^{1/3} p}{(-9q + \sqrt{3}\sqrt{4p^3 + 27q^2})^{1/3}} + \frac{(-9q + \sqrt{3}\sqrt{4p^3 + 27q^2})^{1/3}}{2^{1/3}3^{2/3}}, \\ \beta_2 &= \frac{(KS - 1)}{K} + \frac{(1 + i\sqrt{3})p}{2^{2/3}3^{1/3}(-9q + \sqrt{3}\sqrt{4p^3 + 27q^2})^{1/3}} - \frac{(1 - i\sqrt{3})(-9q + \sqrt{3}\sqrt{4p^3 + 27q^2})^{1/3}}{2 \times 2^{1/3}3^{2/3}}, \\ \beta_3 &= \frac{(KS - 1)}{K} + \frac{(1 - i\sqrt{3})p}{2^{2/3}3^{1/3}(-9q + \sqrt{3}\sqrt{4p^3 + 27q^2})^{1/3}} - \frac{(1 + i\sqrt{3})(-9q + \sqrt{3}\sqrt{4p^3 + 27q^2})^{1/3}}{2 \times 2^{1/3}3^{2/3}} \end{aligned} \quad (20)$$

The boundary value problem (16) has been solved numerically by Khan et al. [35], using Homotopy Perturbation Pade Transformation, and Usafzai et al. [32-34], using the Runge-Kutta-Fehlberg technique, when  $S = K = 0$  and  $\lambda = 1$  (stretching sheet). This is a type of adaptive step size control method that uses a combination of two different Runge-Kutta methods to estimate the solution at each step: a 4<sup>th</sup>- order method and a 5<sup>th</sup>- order method. The Runge-Kutta-Fehlberg method is highly accurate, and its adaptive step size control makes it efficient for solving ordinary differential equations with variable time steps. The comparison of the obtained results for the reduced skin friction  $f''(0)$  is given in Table 1.



**Table 1.** Value of  $f''(0)$  for  $S = K = 0$  and  $\lambda = 1$ .

$\lambda$	Khan et al. [35]	Present result
1.0	-1.414214	-1.414214

**Table 2.** Values of  $-\theta'$  for several values of  $Pr$ .

$Pr$	Wang [38]	Gorla and Sidawi [39]	Present results
0.07	0.0656	0.0656	0.0663
0.20	0.1691	0.1691	0.1691
0.70	0.4539	0.5349	0.4539
2.00	0.9114	0.9114	0.9113
7.00	1.8954	1.8905	1.8954
20.00	3.3539	3.3539	3.3539
70.00	6.4622	6.4622	6.4621

**3.2. Case  $K = 0$**

The boundary value problem (16), reduces to:

$$f''' + ff'' - f'^2 = 0, \quad f(0) = S, \quad f'(0) = \lambda, \quad f'(\eta) \rightarrow 0 \text{ as } \eta \rightarrow \infty \tag{21}$$

and has the following exact analytical solution (see Rosca and Pop [36]):

$$f(\eta) = S + \frac{\lambda}{\beta} (1 - e^{-\beta \eta}), \quad \beta = (S + \lambda) > 0 \tag{22}$$

It gives:

$$\beta^2 - S\beta - \lambda = 0 \tag{23}$$

and then:

$$\beta = \frac{1}{2} (S + \sqrt{S^2 + 4\lambda}) \tag{24}$$

so that:

$$f''(0) = -\lambda \beta \tag{25}$$

Thus, we obtain from (24), as anticipated,  $\lambda_c < -S^2/4$ , where  $\lambda_c < 0$  is the critical value of  $\lambda < 0$ , for which the boundary value problem (21) has physically realizable solutions in practice. We observe that when  $\lambda = 1$  (stretching sheet),  $S = 0$  and  $\beta = 1$ , it results in from (25) that  $f''(0) = -1$ , which agrees with the solution obtained by Crane [37] for the first time.

Further, Eq. (9) along with the boundary conditions (12) for  $\theta(\eta)$ , reduce to the following boundary value problem:

$$\theta'' + Pr f \theta' = 0, \quad \theta(0) = 1, \quad \theta(\eta) \rightarrow 0 \text{ as } \eta \rightarrow \infty \tag{26}$$

This boundary value problem has been solved both analytical and numerically by Usafzai et al. [34, 35]. It has the following closed analytical solution:

$$\theta(\eta) = 1 - \frac{\int_0^\eta \exp \left\{ -Pr \int_0^S \left[ S + \frac{A\lambda}{\sqrt{A + \sigma\beta^2}} (1 - \exp(-\beta\eta/\sqrt{A})) \right] dS \right\} d\eta}{\int_0^\infty \exp \left\{ -Pr \int_0^S \left[ S + \frac{A\lambda}{\sqrt{A + \sigma\beta^2}} (1 - \exp(-\beta\eta/\sqrt{A})) \right] dS \right\} d\eta} \tag{27}$$

with

$$\theta'(0) = - \frac{1}{\int_0^\infty \exp \left\{ -Pr \int_0^S \left[ S + \frac{A\lambda}{\sqrt{A + \sigma\beta^2}} (1 - \exp(-\beta\eta/\sqrt{A})) \right] dS \right\} d\eta} \tag{28}$$

The results for the reduced Nusselt number  $-\theta'(0)$ , are compared with those obtained by Wang [38], and Gorla and Sidawi [39], for several values of the Prandtl number  $Pr$ , are given in Table 2.

It can be seen, from Tables 1 and 2, that the present results, are in excellent agreement, with those by Wang [38] and Gorla and Sidawi [39]. It conforms that the present results are accurate and correct.

The next results are given for the boundary value problem (16). The variation of  $\beta$  curves against several values of suction/injection  $S$ , stretching/shrinking  $\lambda$  and slip  $K$  parameters, are shown in Figs. 2 and 3. It is seen that unique solution exist for  $\beta$  values when  $-10.3 \leq S \leq 10$ , triple solutions exist (upper and lower branch solutions) for  $\beta$  when  $-13 \leq S \leq 10$  (Fig. 2),  $-6 \leq \lambda \leq 6$  and  $0 \leq K \leq 5$  (Fig. 3).

The reduced skin friction profiles  $-f''(0)$  against (a)  $\lambda$  when  $S = 1.1, 1.2$  and  $1.3$ , and against (b)  $K$  when  $0.0 \leq K \leq 2.6$  are presented in Figs. 4 and 5, where triple (upper and lower branch) solutions are depicted, for  $\lambda_c = -0.451688 \leq \lambda \leq 2.0$  (Fig. 5a) and  $K_c = 0.592233 \leq 2.6$  (Fig. 5b), where  $S_c, \lambda_c$  and  $K_c$  are the critical value of  $S, \lambda$  and  $K$  for which the boundary value problem (16) possess physically solutions applicable in practice. However, for  $\lambda \leq \lambda_c = -0.451688 < 0$  and  $0.59222333 \leq K_c$ , the boundary value problem (16) has no solutions and the full partial differentiations equations (1) to (5) along with the boundary conditions (6) needs to be solved numerically.

Figures 6 and 7 show how the velocity profiles  $f'(\eta)$  are varying. It is obvious that the far field boundary conditions in (12) are approached asymptotically as  $\eta \rightarrow \infty$ , which is an excellent indicator that our numerical results are correct. We observe from these graphs that the upper branch solution of  $f'(\eta)$  presents a thickness of the boundary layer, which is thinner than the one observed for the second solution (lower branch solution).



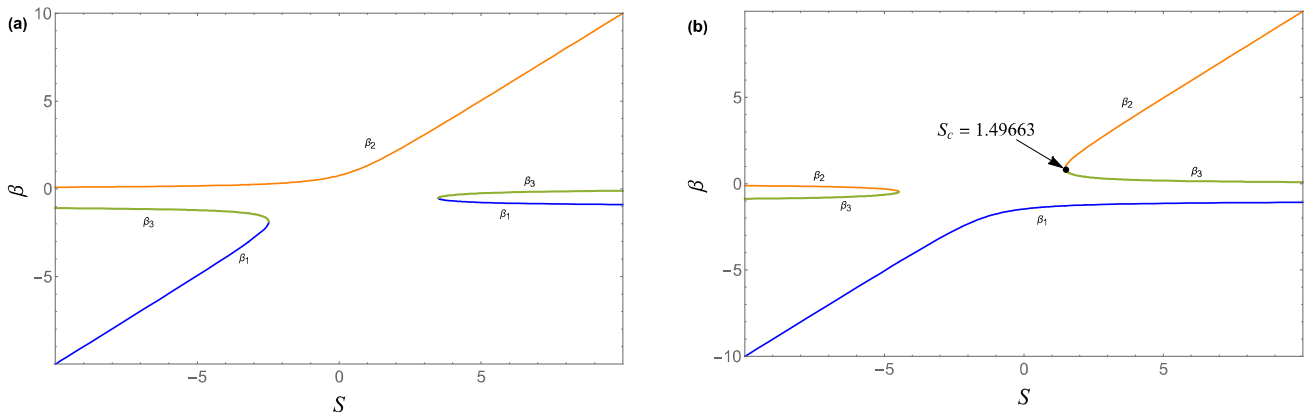


Fig. 2. The variation of  $\beta$  curves against  $S$  for the (a) stretching sheet  $\lambda > 0$  and (b) the shrinking sheet  $\lambda < 0$ .

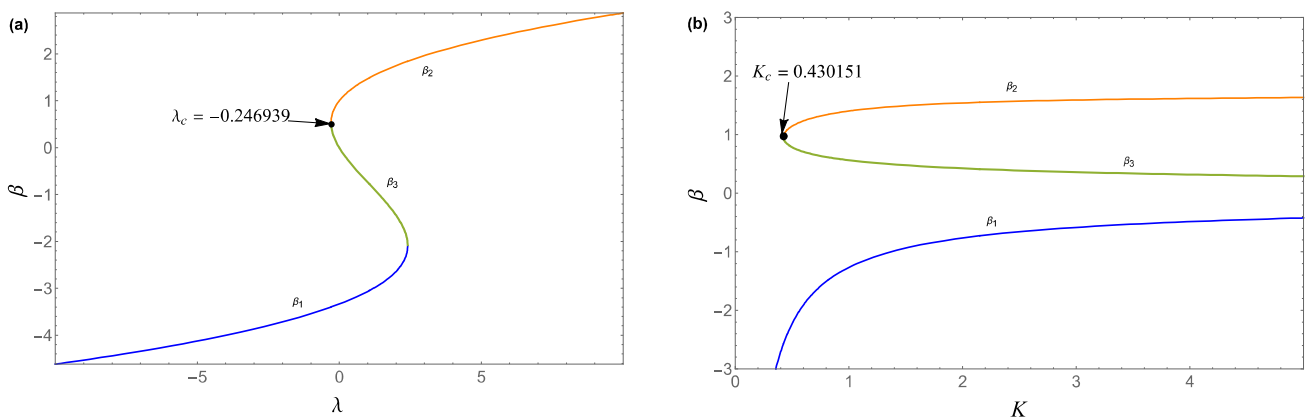


Fig. 3. The variation of  $\beta$  curves against (a) the stretching/shrinking strength parameter  $\lambda$  and (b) against  $K$  for the shrinking sheet  $\lambda < 0$ .

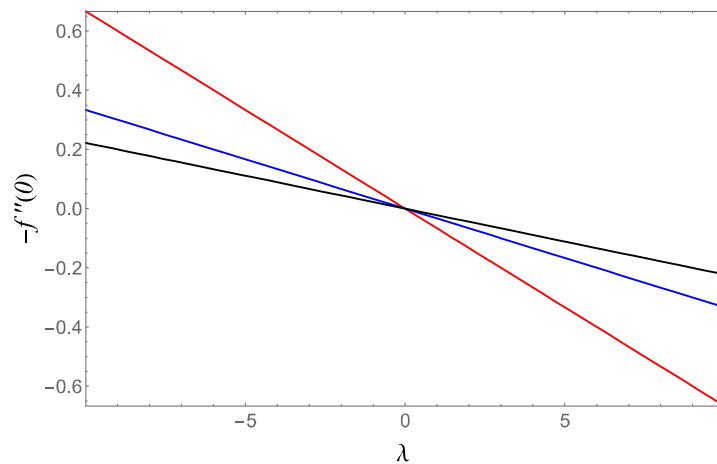


Fig. 4. Reduced skin friction profiles  $-f''(0)$  against  $\lambda$  when  $K = 1, 2$  and  $3$ .

#### 4. Conclusions

The steady gyrostatic nanofluid past a permeable stretching/shrinking sheet with slip condition using the nanofluid model proposed by Buongiorno, were performed by analytical/numerical solutions. The triple-nature solutions for  $\beta$ ,  $f''(0)$  and  $f'(\eta)$  were obtained numerically with respect to the involved parameters: suction/injection  $S$ , stretching/shrinking  $\lambda$  and slip  $K$ , are analyzed in details and presented in 2 tables and 7 figures, which define the solutions domains for existence of unique or multiple (three) solutions. These are key considerations of this analysis. The numerical method has several advantages in terms of speed of convergence and cost of implementation and they can contribute to other researchers on finding approximate solutions of practical problems in the modern industry.



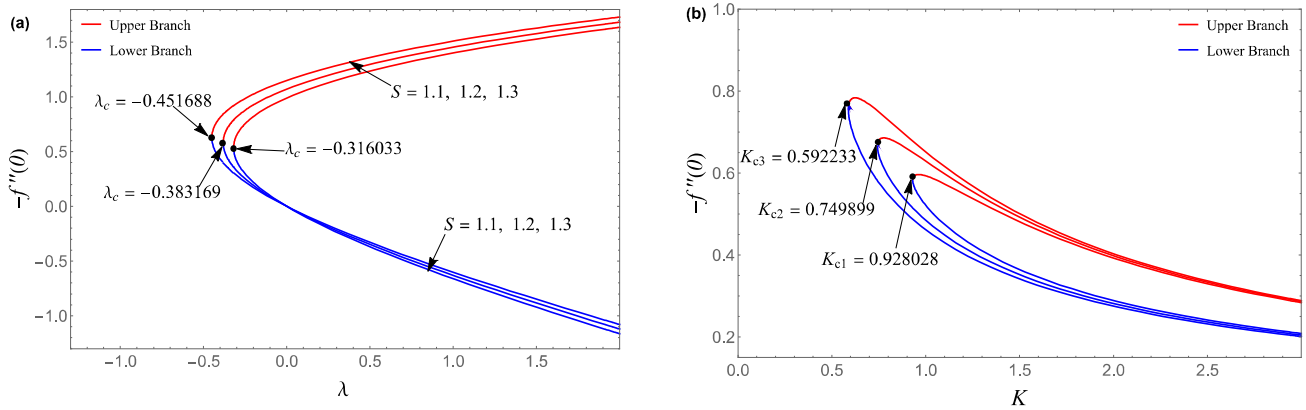


Fig. 5. Reduced skin friction profiles  $-f''(0)$  against (a)  $\lambda$  when  $S = 1.1, 1.2,$  and  $1.3$  and against (b)  $K$  when  $0.0 \leq K \leq 2.6$ .

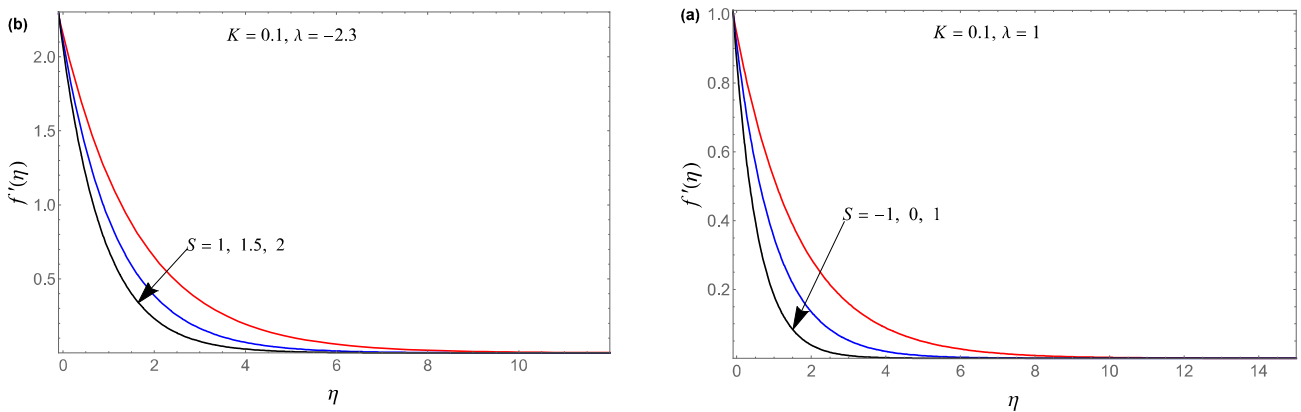


Fig. 6. Velocity profiles  $f'(\eta)$  for (a)  $K = 0.1, \lambda = 1$  (stretching sheet) and  $S = -1, 0$  and  $1$  (b)  $K = 0.1, \lambda = -2.3$  (shrinking sheet) and  $S = 1, 1.5$  and  $2$ .

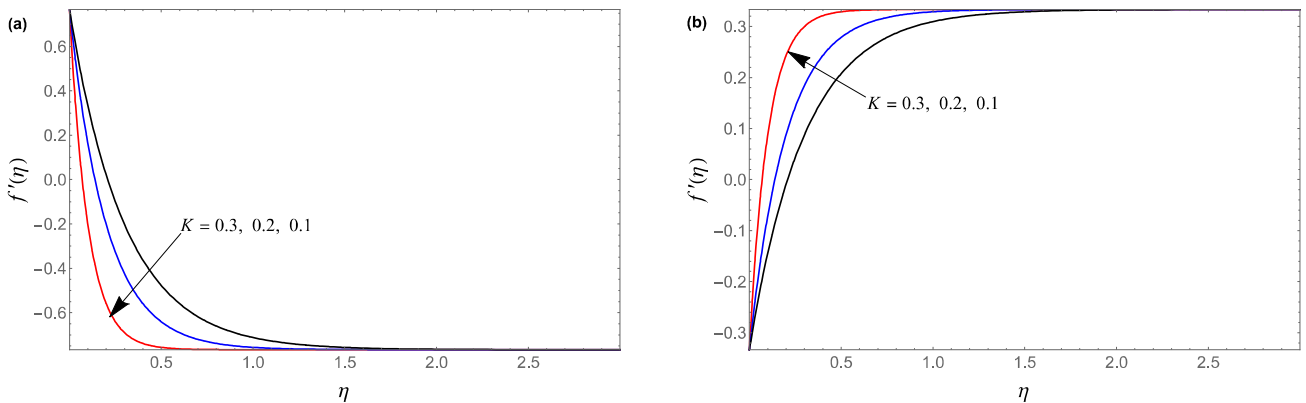


Fig. 7. Velocity profiles  $f'(\eta)$  against (a)  $K$  when  $\lambda = 2.3$  and against (b)  $K$  when  $\lambda = -2.3$ .

### Author Contributions

Methodology validation, investigation, visualization, Waqar Khan Usafzai; Conceptualization, formal analysis, data curation, writing original draft preparation, supervision, Ioan Pop; data curation, writing-original draft preparation, writing-review and editing, supervision, Emad H. Aly. All authors have read and agreed to the published version of the paper.

### Acknowledgments

The authors would like to thank two anonymous reviewers for their valuable suggestions and comments. They would also like to thank the editor for his suggestions.

### Conflict of Interest

The authors declared no potential conflicts of interest concerning the research, authorship, and publication of this article.



## Funding

The work of Waqar Khan Usafzai has been supported by Nanjing Institute of Technology, Nanjing, China under Grant No. YKJ202126. The work of Ioan Pop has been supported from the Grant PN-III-P4-PCE-2021-0993, UEFISCDI, Romania.

## Data Availability Statements

Data and codes that support the findings of this study are available from the corresponding author upon reasonable request.

## References

- [1] Choi, S.U.S., Enhancing thermal conductivity of fluids with nanoparticles, In: *Proceedings of the 1995 ASME International Mechanical Engineering Congress and Exposition*, FED 231/MD 66, 99–105, 1995.
- [2] Shah, F., Khan, S.A., Al-Khaled, K., Khan, M.I., Khan, S.U., Shah, N.A., Ali, R., Impact of entropy optimized Darcy-Forchheimer flow in MnZnFe2O4 and NiZnFe2O4 hybrid nanofluid towards a curved surface, *ZAMM Zeitschrift für Angewandte Mathematik und Mechanik*, 102, 2022, e202100194.
- [3] Raza, A., Al-Khaled, K., Muhammad, T., Khan, S.U., Accelerating flow of carbon nanotubes with carboxymethyl cellulose and blood base materials with comparative thermal features: Prabhakar fractional model, *Mathematical Problems in Engineering*, 2023, 2023, 3468295.
- [4] Khan, S.U., Ali, H.M., Swimming of gyrotactic microorganisms in unsteady flow of Eyring Powell nanofluid with variable thermal features: Some bio-technology applications, *International Journal of Thermophysics*, 44, 2023, 151.
- [5] Ahmad, H., Al-Khaled, K., Sowayan, A.S., Abdullah, M., Hussain, M., Hammad, A., Khan, S.U., Thili, I., Experimental investigation for automotive radiator heat transfer performance with ZnO-Al2O3/water based hybrid nanoparticles: An improved thermal model, *International Journal of Modern Physics B*, 37(05), 2023, 2350050.
- [6] Mahian, O., Kolsi, L., Amani, M., Estellé, P., Ahmadi, G., Kleinstreuer, C., Marshall, J.S., Siavashi, M., Taylor, R.A., Niazmand, H., Wongwises, S., Hayat, T., Kolanjiyil, A., Kasaeian, A., Pop, I., Recent advances in modeling and simulation of nanofluid flows—Part I: Fundamentals and theory, *Physics Reports*, 790, 2019, 1-48.
- [7] Mahian, O., Kolsi, L., Amani, M., Estellé, P., Ahmadi, G., Kleinstreuer, C., Marshall, J.S., Taylor, R.A., Abu-Nada, E., Rashidi, S., Niazmand, H., Wongwises, S., Hayat, T., Kasaeian, A., Pop, I., Recent advances in modeling and simulation of nanofluid flows—Part II: Applications, *Physics Reports*, 791, 2019, 1-59.
- [8] Pop, I., Groşan, T., Revnic, C., Rosca, A., Unsteady flow and heat transfer of nanofluids, hybrid nanofluids, micropolar fluids and porous media: a review, *Thermal Science and Engineering Progress*, 46, 2023, 102248.
- [9] Minea, A.A., *Advances in New Heat Transfer Fluids: From Numerical to Experimental Techniques*, CRC Press, Taylor & Francis Group, New York, 2017.
- [10] Merkin, J.H., Pop, I., Lok, Y.Y., Grosan, T., *Similarity Solutions for the Boundary Layer Flow and Heat Transfer of Viscous Fluids, Nanofluids, Porous Media and Micropolar Fluids*, Elsevier, Oxford, UK, 2021.
- [11] Buongiorno, J., Convective transport in nanofluids, *ASME Journal of Heat Transfer*, 128, 2006, 240-250.
- [12] Pedley, T.J., Hill, N.A., Kessler, J.O., The growth of bioconvection patterns in a uniform suspension of gyrotactic micro-organisms, *Journal of Fluid Mechanics*, 195, 1988, 223–237.
- [13] Kuznetsov, A.V., Geng, P., The interaction of bioconvection caused by gyrotactic micro-organisms and settling of small solid particles, *International Journal of Numerical Methods for Heat & Fluid Flow*, 15, 2005, 328-347.
- [14] Kuznetsov, A.V., Avramenko, A.A., Effect of small particles on this stability of bioconvection in a suspension of gyrotactic microorganisms in a layer of finite depth, *International Communications in Heat and Mass Transfer*, 31, 2004, 1-10.
- [15] Kuznetsov, A.V., The onset of nanofluid bioconvection in a suspension containing both nanoparticles and gyrotactic microorganisms, *International Journal of Heat and Mass Transfer*, 37, 2010, 1421-1425.
- [16] Kuznetsov, A.V., Non-oscillatory and oscillatory nanofluid bio-thermal convection in a horizontal layer of finite depth, *European Journal of Mechanics - B/Fluids*, 30, 2011, 156-165.
- [17] Aziz, A., Khan, W.A., Pop, I., Free convection boundary layer flow past a horizontal flat plate embedded in porous medium filled by nanofluid containing gyrotactic microorganisms, *International Journal of Thermal Sciences*, 56, 2012, 48-57.
- [18] Tham, L., Nazar, R., Pop, I., Mixed convection flow over a solid sphere embedded in a porous medium filled by a nanofluid containing gyrotactic microorganisms, *International Journal of Heat and Mass Transfer*, 62, 2013, 647-660.
- [19] Xu, H., Pop, I., Mixed convection flow of a nanofluid over a stretching surface with uniform free stream in the presence of both nanoparticles and gyrotactic microorganisms, *International Journal of Heat and Mass Transfer*, 75, 2014, 610-623.
- [20] Fisher, E.G., *Extrusion of Plastics*, Wiley, New York, 1976.
- [21] Miklavcic, M., Wang, C.Y., Viscous flow due to a shrinking sheet, *Quarterly of Applied Mathematics*, 64, 2006, 283-290.
- [22] Fang, T., Yao, S., Zhang, J., Aziz, A., Viscous flow over a shrinking sheet with a second order slip flow model, *Communications in Nonlinear Science and Numerical Simulation*, 15, 2010, 1831-1842.
- [23] Rohni, A., Ahmad, S., Ismail, A.I., Pop, I., Flow and heat transfer over an unsteady shrinking sheet with suction in a nanofluid using Buongiorno's model, *International Communications in Heat and Mass Transfer*, 43, 2013, 75-80.
- [24] Aman, F., Khazim, W.H.W.M., Mansur, S., Mixed convection flow of a nanofluid containing gyrotactic microorganisms over a stretching/shrinking sheet in the presence of magnetic field, *Journal of Physics: Conference Series*, 890, 2017, 012027.
- [25] Goldstein, J., On backward boundary layers and flow in converging passages, *Journal of Fluid Mechanics*, 21, 1965, 33-45.
- [26] Al-Zubaidi, A., Abutuqayqah, H., Ahmad, B., Bibi, S., Abbas, T., Saleem, S., Analysis of slip condition in MHD nanofluid flow over stretching sheet in presence of viscous dissipation: Keller box simulations, *Alexandria Engineering Journal*, 82, 2023, 26-34.
- [27] Mabood, F., Usman, H., Multiple slips effects on MHD thermo-solute flow in porous media saturated by nanofluid, *Mathematical Modelling of Engineering Problems*, 6, 2019, 502-510.
- [28] Navier, C.L., M'emoire sur les lois du mouvement des fluides, *Mem. Acad. R. Sci.*, 6, 1823, 389-440.
- [29] Maxwell, C.J., On stresses in rarefied gasses arising from inadequacies of temperature, *Philosophical Transactions of the Royal Society A*, 170, 1897, 231-256.
- [30] Von Smoluchowski, M., Ueber wärmeleitung in verdünnten gasen, *Annalen der Physik und Chemie*, 64, 1898, 1013.
- [31] Ahmed, N., Tassaddiq, A., Alabdian, R., Adnan, K.U., Noor, S., Mohyud-Din, S.T., Khan, I., Applications of Nanofluids for the Thermal Enhancement in Radiative and Dissipative Flow over a Wedge, *Applied Sciences*, 9(10), 2019, 1976.
- [32] Usafzai, W.K., Aly, E.H., Exact multiple solutions of 2-D bidirectional moving plate micropolar hybrid nanofluid flow with heat transfer, *Chinese Journal of Physics*, 80, 2022, 414-426.
- [33] Usafzai, W.K., Aly, E.H., Tharwat, M.M., Mahros, A.M., Modelling of micropolar nanofluid flow over a flat surface with slip velocity and heat transfer: Exact multiple solutions, *Alexandria Engineering Journal*, 75, 2023, 313-323.
- [34] Usafzai, W.K., Saeed, A.M., Aly, E.H., Puneeth, V., Pop, I., Wall jet nanofluid flow with thermal energy and radiation in the presence of power-law, *Numerical Heat Transfer, Part A: Applications*, 2023, <https://doi.org/10.1080/10407782.2023.2222456>.
- [35] Khan, M., Gondal, M.A., Homotopy perturbation Padé transform method for Blasius flow equation using He's polynomials, *International Journal of Nonlinear Sciences and Numerical Simulation*, 12, 2011, 1-7.
- [36] Rosca, N.C., Pop, I., Unsteady boundary layer flow over a permeable curved stretching/shrinking surface, *European Journal of Mechanics - B/Fluids*, 51, 2015, 61-67.
- [37] Crane, L.J., Flow past a stretching plate, *Zeitschrift für Angewandte Mathematik und Physik*, 21, 1970, 645-647.
- [38] Wang, C.Y., Free convection on a vertical stretching surface, *ZAMM Zeitschrift für Angewandte Mathematik und Mechanik*, 69, 1989, 418-420.
- [39] Gorla, R.S.R., Sidawi, I., Free convection on a vertical stretching surface with suction and blowing, *Applied Scientific Research*, 52, 1994, 247-257.



**ORCID iD**

Ioan Pop  <https://orcid.org/0000-0002-0660-6543>



© 2024 Shahid Chamran University of Ahvaz, Ahvaz, Iran. This article is an open access article distributed under the terms and conditions of the Creative Commons Attribution-NonCommercial 4.0 International (CC BY-NC 4.0 license) (<http://creativecommons.org/licenses/by-nc/4.0/>).

**How to cite this article:** Usafzai W.K., Pop I., Aly E.H. Steady Gyrostatic Nanofluid Flow past a Permeable Stretching/shrinking Sheet with Velocity Slip Condition using the Nanofluid Model Proposed by Buongiorno, *J. Appl. Comput. Mech.*, 10(2), 2024, 413-421. <https://doi.org/10.22055/jacm.2024.45412.4362>

**Publisher's Note** Shahid Chamran University of Ahvaz remains neutral with regard to jurisdictional claims in published maps and institutional affiliations.

